Synthesis and Characterization of Three New Rare-Earth Titanium Oxyselenides: $Ln_{3.67}Ti_2O_3Se_6$ (Ln = Ce, Nd, Sm)

Olivier Tougait and James A. Ibers*

Department of Chemistry, Northwestern University, 2145 Sheridan Road, Evanston, Illinois 60208-3113

Received March 6, 2000. Revised Manuscript Received June 20, 2000

Three new compounds, $Ln_{3.67}Ti_2O_3Se_6$ (Ln = Ce, Nd, Sm), have been prepared from the reaction in stoichiometric ratios of Ln, TiO_2, Ti, and Se in sealed fused-silica tubes at 950 °C. A KBr flux was used to promote the crystal growth. Single-crystal X-ray diffraction measurements show that these compounds are isostructural. They crystallize with four formula units in the monoclinic space group *C*2/*m* in a new structure type that contains four crystallographically independent Ln atoms with three different coordination geometries and three nonequivalent Ti atoms in octahedral geometry. The structure comprises infinite condensed slabs of composition $^2_\infty[Ln_4Ti_2O_4Se_4Se_{5/2}]$ alternating along the *a* axis with extended slabs of composition $^2_\infty[Ln_{3.33}Ti_2O_2Se_3Se_{5/2}]$. To achieve charge balance, Ti^{3+} and Ti^{4+} cations must be present in equal numbers; these are randomly distributed over the Ti sites. Crystal data at −120 °C follow: $Ce_{3.67}Ti_2O_3Se_6$, a = 28.315(6) Å, b = 3.8719(8) Å, c = 11.271(2) Å, β = 90.45(3)°, $R(F)$ = 0.0286; $Nd_{3.67}Ti_2O_3Se_6$, a = 28.121(6) Å, b = 3.8232(8) Å, c = 11.179(2) Å, β = 90.15(3)°, $R(F)$ = 0.0322; $Sm_{3.67}Ti_2O_3Se_6$, a = 27.961(6) Å, b = 3.7827(8) Å, c = 11.128(2) Å, β = 90.26(3)°, $R(F)$ = 0.0294. The magnetic susceptibilities of the $Ln_{3.67}Ti_2O_3Se_6$ (Ln = Ce, Nd, Sm) compounds are dominated by the trivalent rare-earth cations and display paramagnetic behavior down to 5 K.

Introduction

The solid-state chemistry of quaternary oxychalcogenides involving both a d- and an f-block element has not been explored extensively. Most of the known examples incorporate an amazing range of compositions and involve the light lanthanides (La, Ce, Pr, Nd, Sm) and Group 4, 5, or 6 d-block metals. These include $LnCrOQ_2$ (Q = S and Ln = La, Ce, Pr, Nd, Sm[1−4]; Q = Se and Ln = La, Ce, Nd),[5,6] $Ln_5V_3O_7S_6$ (Ln = La, Ce, Pr, Nd),[7,8] $Ln_2Ta_3O_8Se_2$ (Ln = La, Ce, Pr, Nd),[9] $La_6Ti_2O_5S_8$,[10] $La_4Ti_3O_8S_4$,[10] $Ln_{20}Ti_{11}O_6S_{44}$ (Ln = La, Ce),[11,12] $La_{14}Ti_8O_6S_{33}$,[13] $La_8Ti_{10}O_4S_{24}$,[14] $La_{8+x}Ti_{8+y}O_4S_{24}$ ($x + y \leq 2$),[15] $Sm_3NbO_4Se_3$,[16] and $Ln_2Ti_2O_5S_2$ (Ln = Pr, Nd, Sm).[17]

The main features of these compounds are strong ionic behavior and the formation of three-dimensional crystal structures by face- and edge-sharing of polyhedra, leading to very stable materials, none of which is known to melt below 1200 °C. As there are no Q−Q bonds in these systems, the oxidation states of the cations can be readily assigned: the rare-earth elements are trivalent and all valence electrons are involved in the M−Q bonds, where M is the d-block metal. However, some of these are mixed-valence compounds. Thus, $La_5V_3O_7S_6$[7,8] contains both V^{3+} and V^{4+} sites, $Ln_2Ta_3O_8Se_2$[9] contains both Ta^{4+} and Ta^{5+} sites, and $La_{14}Ti_8O_6S_{33}$,[13] $La_{8+x}Ti_{8+y}O_4S_{24}$,[15] and $La_8Ti_{10}O_4S_{24}$[14] contain both $Ti^{3+}$and Ti^{4+} cations. Among these compounds only $Ln_2Ta_3O_8Se_2$ exhibits separate M^{n+} and M^{m+} sites, as determined crystallographically and confirmed by band structure calculations.[18] All the others have indistinguishable mixed-valence d-cations

(1) Dugué, J.; Vovan, T.; Villers, J. *Acta Crystallogr., Sect. B* **1980**, *36*, 1291−1294.
(2) Dugué, J.; Vovan, T.; Villers, J. *Acta Crystallogr., Sect. B* **1980**, *36*, 1294−1297.
(3) Wintenberger, M.; Vovan, T.; Guittard, M. *Solid State Commun.* **1985**, *53*, 227−230.
(4) Vovan, T.; Dugué, J.; Guittard, M. *Mater. Res. Bull.* **1978**, *13*, 1163−1166.
(5) Wintenberger, M.; Dugué, J.; Guittard, M.; Dung, N. H.; Tien, V. V. *J. Solid State Chem.* **1987**, *70*, 295−302.
(6) Van, T. V.; Huy, D. N. *C. R. Acad. Sci., Sér. 2* **1981**, *293*, 933−936.
(7) Dugué, J.; Vovan, T.; Laruelle, P. *Acta Crystallogr., Sect. C* **1985**, *41*, 1146−1148.
(8) Vovan, T.; Dugué, J.; Guittard, M. *C. R. Acad. Sci., Sér. 2* **1981**, *292*, 957−959.
(9) Brennan, T. D.; Aleandri, L. E.; Ibers, J. A. *J. Solid State Chem.* **1991**, *91*, 312−322.
(10) Cody, J. A.; Ibers, J. A. *J. Solid State Chem.* **1995**, *114*, 406−412.
(11) Deudon, C.; Meerschaut, A.; Cario, L.; Rouxel, J. *J. Solid State Chem.* **1995**, *120*, 164−169.
(12) Cody, J. A.; Deudon, C.; Cario, L.; Meerschaut, A. *Mater. Res. Bull.* **1997**, *32*, 1181−1192.
(13) Tranchitella, L. J.; Fettinger, J. C.; Eichhorn, B. W. *Chem. Mater.* **1996**, *8*, 2265−2271.
(14) Cario, L.; Deudon, C.; Meerchaut, A.; Rouxel, J. *J. Solid State Chem.* **1998**, *136*, 46−50.
(15) Tranchitella, L. J.; Fettinger, J. C.; Heller-Zeisler, S. F.; Eichhorn, B. W. *Chem. Mater.* **1998**, *10*, 2078−2085.
(16) Meerschaut, A.; Boyer, C.; Lafond, A.; Cario, L.; Rouxel, J. *J. Solid State Chem.* **1998**, *137*, 122−126.
(17) Goga, M.; Seshadri, R.; Ksenofontov, V.; Gütlich, P.; Tremel, W. *J. Chem. Soc., Chem. Commun.* **1999**, 979−980.
(18) Brennan, T. D.; Ibers, J. A. *J. Solid State Chem.* **1992**, *98*, 82−89.

10.1021/cm000203m CCC: $19.00
Published on Web 08/25/2000

randomly distributed over nonequivalent crystallographic sites.

Here, we present the syntheses, crystal structures, and magnetic properties of three new rare-earth titanium oxyselenides $Ln_{3.67}Ti_2O_3Se_6$ (Ln = Ce, Nd, Sm). By charge balance these are mixed-valence compounds containing equal numbers of Ti^{3+} and Ti^{4+} cations.

Experimental Section

Syntheses. $Sm_{3.67}Ti_2O_3Se_6$ single crystals were first obtained from the reaction of Sm (Alfa, 40 mesh, 99.9%), Ti (Alfa, 100 mesh, 99.9%), and Se (Alfa, 325 mesh, 99.5%) in the ratio 3/1/6 in an unprotected fused-silica tube to which a small amount of I_2 had been added. The reaction tube was sealed at 10^{-4} Torr and then placed in a furnace where it was heated at a rate of 10 °C/h to 1000 °C where it was held for 96 h. Then the furnace was cooled to 700 °C at 3 °C/h when it was turned off. The final product showed mainly golden platelike crystals of $SmSe_3$ and a few black needles (typically 0.3 × 0.02 × 0.02 mm) of what turned out to be $Sm_{3.67}Ti_2O_3Se_6$. The source of oxygen in this compound was undoubtedly the silica tube, which was etched in the reaction.

Powders of $Ln_{3.67}Ti_2O_3Se_6$ (Ln = Ce, Nd, Sm) subsequently have been obtained in a more rational manner from the reactions of 1.554 mmol of Ln (Ce, Alfa, 40 mesh, 99.9%; Nd, Alfa, 40 mesh, 99.9%), 0.635 mmol of TiO_2 (Alfa, 100 mesh, 99.99%), 0.212 mmol of Ti, and 2.541 mmol of Se loaded in unprotected fused-silica tubes. These tubes were sealed at 10^{-4} Torr and heated to 950 °C over 50 h, maintained at this temperature for 96 h, and then cooled to room temperature over a 10-h period. The purity of the samples was established by comparison of their X-ray powder diffraction patterns with the theoretical patterns calculated[19] from their crystal structures. These patterns, which were fully indexed, were obtained on a Rigaku powder diffractometer equipped with monochromatized Cu $K\alpha_1$ radiation.

Single crystals of $Ln_{3.67}Ti_2O_3Se_6$ (Ln = Ce, Nd, Sm) were obtained from these powders, which were re-ground before being loaded into fused-silica tubes to which 150 mg of KBr (Alfa, 99%) had been added to promote crystallization. The reaction tubes were heated at 950 °C for 96 h and then slowly cooled to room temperature. The final products were washed with a water−methanol mixture to remove the KBr flux. Thin black needles were embedded in the powder.

Energy-Dispersive X-ray (EDX) Analysis. EDX analyses were carried out with the use of a 3500N Hitachi SEM. Through the use of the known compounds $LnCrOSe_2$ (Ln = Ce, Nd, Sm),[5,6,20] $Cs_4Ti_3Se_{14}$, and $Cs_2TiCu_2Se_4$[21,22] as external standards, additional corrections were superimposed on the ZAF internal corrections. For three different single crystals from each preparation, the presence of oxygen was systematically detected, but reasonable semiquantitative analysis for this element could not be obtained. EDX results on the heavier elements gave the following average atomic ratios: Ce(35(3)), Ti(17(2)), Se(48(3)); Nd(35(3)), Ti(16(2)), Se(49(2)); Sm(31.5(20)), Ti(15.5(20)), Se(53(3)), in good agreement with the values of Ln(31.5)Ti(17.1)Se(51.4) calculated for the composition $Ln_{3.67}Ti_2Se_6$ (Ln = Ce, Nd, Sm).

Inductively Coupled Plasma (ICP-AES) Analysis. ICP analyses were carried out with the use of a Thermo Jarrell Ash Atomscan Model 25 Sequential ICP Spectrometer. First, 3.8 mg of single crystals of $Nd_{3.67}Ti_2O_3Se_6$ were dissolved in 5 mL of 70% HNO_3. Then the solution was adjusted to 100 mL with deionized water. The concentrations in ppm obtained for the detectable elements Nd, Ti, and Se were 17.5(1), 3.03(1), and 15.7(5), respectively, in excellent agreement with the values of 17.5, 3.2, and 15.7 calculated from the formula $Nd_{3.67}Ti_2O_3Se_6$.

Structural Characterization. Single-crystal X-ray diffraction data were collected on a Bruker Smart 1000 CCD diffractometer at −120 °C with the use of monochromatized Mo Kα radiation. The diffracted intensities generated by a scan of 0.3° in ω were recorded for more than a hemisphere of data on 1878 frames for $Ln_{3.67}Ti_2O_3Se_6$ (Ln = Ce, Sm) and on 1271 frames for $Nd_{3.67}Ti_2O_3Se_6$. The exposure times were 20 s/frame for $Ce_{3.67}Ti_2O_3Se_6$, 15 s/frame for $Sm_{3.67}Ti_2O_3Se_6$, and 25 s/frame for $Nd_{3.67}Ti_2O_3Se_6$. Initial processing of the data with no cell constraints resulted in all interaxial angles being close to 90°. Reciprocal lattice projections along the three axes with the use of XPREP[23] showed a mirror plane perpendicular to b^* but only a 2-fold axis along it, leading to Laue class 2/*m*. For each compound, cell refinement and data reduction were carried out with the use of the program SAINT[23] and a face-indexed absorption correction was made with the use of the program XPREP. Finally, the program SADABS[23] was employed to make incident beam and decay corrections.

The crystal structures were solved in space group *C*2/*m*. The positions of the heavy atoms (Ln, Se, Ti) were determined by direct methods with the program SHELXS of the SHELXTL-PC suite of programs[24] and the positions of the O atoms were located from successive difference electron density syntheses. All structures were refined by full-matrix least-squares techniques with the use of the program SHELXL.[24] The resultant displacement ellipsoids for the Ln(4) site were excessively large, indicating that there was less electron density at this site than that assumed in the model. This electron density can be modeled in at least three ways: (1) assume that only Ln atoms occupy the Ln(4) site and allow the occupancy at this site to vary; or assume that the Ln(4) site is randomly occupied by both Ln and Ti atoms and (2) keep full occupancy or (3) vary the occupancy at this site. In all three models charge neutrality of the overall composition is maintained. Models (2) and (3) are considered since it was reported recently[15] that La and Ti cations in a mixed octahedral environment of O and S atoms can be statistically disordered over the same crystallographic site. Models (2) and (3) differ conceptually in the oxidation state of Ti involved, although the X-ray experiment is insensitive to that oxidation state. In simplest terms, we interpret model (2) as involving a mix of Ln^{3+} and Ti^{3+} and model (3) as involving a mix of Ln^{3+} and Ti^{4+}at the Ln(4) site. Calculations carried out for the Ce compound led to similar agreement indices and residual electron densities for all three models. The resultant chemical formulas are as follows: model (1), $Ce_{3.67}Ti_2O_3Se_6$; model (2), $Ce_{3.5}Ti_{2.5}O_3Se_6$; model (3), $Ce_{3.54}Ti_{2.32}O_3Se_6$. The first formula is in better agreement with the EDX and ICP measurements.

The first model, which involves only Ln atoms at the Ln(4) site, also makes better physical sense. The environment around Ln(4) is that of seven Se atoms in a pseudo-octahedral geometry, a common one in rare-earth selenides,[25,26] but to our knowledge an environment never reported for Ti in a chalcogenide. Disorder of a large cation (ionic radius Ce^{3+} = 1.07 Å) and a small cation (ionic radii Ti^{3+} = 0.67 Å and Ti^{4+} = 0.605 Å)[27] at the Ln(4) site, as in models (2) and (3), should lead to Ce−Se distances that are shorter than normal. But the mean Ce(4)−Se distance is 3.041(2) Å, which corresponds well to that of 3.05 Å from the sum of the ionic radii.[27]

Consequently, when model (1) was assumed for all three compounds, the resultant compositions were $Ce_{3.688(2)}Ti_2O_3Se_6$, $Nd_{3.713(2)}Ti_2O_3Se_6$, and $Sm_{3.643(2)}Ti_2O_3Se_6$. Final refinements

(19) Yvon, K.; Jeitschko, W.; Parthé, E. *J. Appl. Crystallogr.* **1977**, *10*, 73−74.
(20) Tougait, O.; Ibers, J. A., unpublished results.
(21) Sunshine, S. A.; Kang, D.; Ibers, J. A. *J. Am. Chem. Soc.* **1987**, *109*, 6202−6204.
(22) Huang, F. Q.; Ibers, J. A., unpublished results.
(23) SMART Version 5.054 Data Collection and SAINT-Plus Version 6.02A Data Processing Software for the SMART System; Bruker Analytical X-ray Instruments, Inc., Madison, WI, 2000.
(24) Sheldrick, G. M. SHELXTL DOS/Windows/NT Version 5.10; Bruker Analytical X-ray Instruments, Inc., Madison, WI, 1997.
(25) Flahaut, J. In *Handbook on the Physics and Chemistry of Rare Earths*; Gschneidner, K. A., Jr., Eyring, L. R., Eds.; North-Holland: New York, 1979; Vol. 4, pp 1−88.
(26) Range, K.-J.; Leeb, R. *Z. Naturforsch., B: Anorg. Chem., Org. Chem.* **1976**, *31*, 685−686.
(27) Shannon, R. D. *Acta Crystallogr., Sect. A* **1976**, *32*, 751−767.

Table 1. X-ray Crystallographic Details

formula	$Ce_{3.67}Ti_2O_3Se_6$	$Nd_{3.67}Ti_2O_3Se_6$	$Sm_{3.67}Ti_2O_3Se_6$
crystal symmetry	monoclinic	monoclinic	monoclinic
space group	*C*2/*m*	*C*2/*m*	*C*2/*m*
a (Å)	28.315(6)	28.121(6)	27.961(6)
b (Å)	3.8719(8)	3.8232(8)	3.7827(8)
c (Å)	11.271(2)	11.179(2)	11.128(2)
β (°)	90.45(3)	90.15(3)	90.26(3)
T (°C)	−120	−120	−120
Z	4	4	4
d_{calc} (g cm^{-3})	6.097	6.353	6.614
μ (cm^{-1})	321.8	350.5	379.2
no. of meas. reflections	5675	3872	5380
R_{int}	0.0259	0.0215	0.0243
no. of unique reflections	1705	1617	1589
$R(F)^a$	0.0286	0.0322	0.0294
$Rw(Fo^2)^b$	0.0604	0.0705	0.0607

[a] $R(F) = \Sigma||F_o| - |F_c|| \Sigma|F_c|$. [b] $Rw(F_o^2) = [\Sigma w(F_o^2 - F_c^2)^2 / \Sigma w F_o^4]^{1/2}$ where $w = 1/[\sigma^2(F_o^2) + (0.04F_o^2)^2]$ for $F_o^2 \geq 0$.

carried out with the occupancy of the Ln(4) site fixed at 0.667, i.e., composition $Ln_{3.67}Ti_2O_3Se_6$, did not differ significantly from those for model (1) in which the occupancy of the site was varied. This final model assumes random occupancy of Ln atoms at two-thirds of the Ln(4) site and requires equal numbers of Ti^{3+} and Ti^{4+} cations in the cell. Crystallographic details are given in Table 1. Further details may be found in the Supporting Information.

Magnetic Measurements. Magnetic measurements on powders were carried out with a SQUID magnetometer (MPMS5, Quantum Design). The samples, 48.0 mg of $Ce_{3.67}Ti_2O_3Se_6$, 25.7 mg of $Nd_{3.67}Ti_2O_3Se_6$, and 47.3 mg of $Sm_{3.67}Ti_2O_3Se_6$, were loaded in gelatin capsules. In the temperature range 5−300 K zero-field cooled (ZFC) measurements were processed for $Ln_{3.67}Ti_2O_3Se_6$ (Ln = Ce, Sm) with 100 G applied field and for $Nd_{3.67}Ti_2O_3Se_6$ both ZFC and field cooled (FC) measurements were processed with 5000 G applied field. Magnetization versus magnetic field data up to 5 T were also collected at 5 K for the Nd compound. All data were corrected for electron core diamagnetism.[28]

Results and Discussion

Syntheses. The new compound $Sm_{3.67}Ti_2O_3Se_6$ was obtained accidentally at first from the reaction of Sm, Ti, and Se in an unprotected fused-silica tube. The compounds $Ln_{3.67}Ti_2O_3Se_6$ (Ln = Ce, Nd, Sm) have been obtained as single phases in a rational manner from the reactions of Ln, Ti, TiO_2, and Se at 950 °C and single crystals have been obtained with the use of a KBr flux.

Crystal Structure Description. The new compounds $Ln_{3.67}Ti_2O_3Se_6$ (Ln = Ce, Nd, Sm) are isostructural and crystallize in a new structure type. The crystal structure of $Ce_{3.67}Ti_2O_3Se_6$ viewed down the *b* axis is displayed in Figure 1. A selection of interatomic distances is provided in Table 2. The four independent Ln atoms are found in three different coordination polyhedra. Atoms Ln(1) and Ln(2) are in a bicapped trigonal prismatic environment (LnO_3Se_5) (Figure 2a); atom Ln(3) is in a tricapped trigonal prismatic environment (LnO_3Se_6) (Figure 2b); Ln(4) is in a seven-coordinate environment ($LnSe_7$), with four Se atoms in an equatorial plane and three other Se atoms in a perpendicular plane, an arrangement usually described as a 7-octahedron with one apex split into two positions (Figure 2c). The three independent Ti atoms are octahedrally coordinated. Each has four Se atoms forming the pseudoequatorial plane, with one trans O atom and one trans Se around atom Ti(1) ($TiOSe_5$) and two trans O atoms around atoms Ti(2) and Ti(3) (TiO_2Se_4) (Figure 2d).

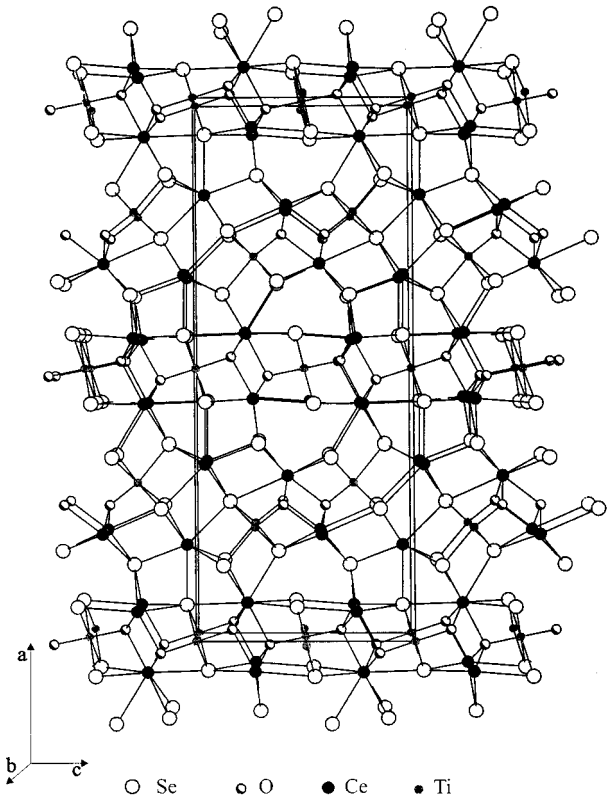

Figure 1. View of the unit cell of $Ce_{3.67}Ti_2O_3Se_6$ along the *b* axis.

Table 2. Selected Interatomic Distances (Å)

distance	$Ce_{3.67}Ti_2O_3Se_6$	$Nd_{3.67}Ti_2O_3Se_6$	$Sm_{3.67}Ti_2O_3Se_6$
Ln(1)−O(3) ×2	2.374(3)	2.341(3)	2.311(3)
Ln(1)−O(1)	2.466(5)	2.445(6)	2.434(6)
Ln(1)−Se(4) ×2	3.040(1)	3.010(1)	2.984(1)
Ln(1)−Se(1)	3.072(1)	3.049(1)	3.042(1)
Ln(1)−Se(5) ×2	3.148(1)	3.117(1)	3.095(1)
Ln(2)−O(2) ×2	2.412(3)	2.380(3)	2.353(3)
Ln(2)−O(2)	2.510(5)	2.482(6)	2.462(5)
Ln(2)−Se(4) ×2	3.001(1)	2.970(1)	2.951(1)
Ln(2)−Se(3) ×2	3.112(1)	3.076(1)	3.054(1)
Ln(2)−Se(6)	3.286(1)	3.292(1)	3.278(1)
Ln(3)−O(1) ×2	2.418(3)	2.380(3)	2.353(3)
Ln(3)−O(3)	2.523(5)	2.490(6)	2.485(5)
Ln(3)−Se(2) ×2	3.120(1)	3.092(1)	3.064(1)
Ln(3)−Se(5)	3.158(1)	3.134(1)	3.121(1)
Ln(3)−Se(3)	3.201(1)	3.193(1)	3.179(1)
Ln(3)−Se(1) ×2	3.224(1)	3.189(1)	3.164(1)
Ln(4)−Se(2) ×2	2.900(1)	2.864(1)	2.839(1)
Ln(4)−Se(4)	2.941(1)	2.917(1)	2.906(1)
Ln(4)−Se(6) ×2	3.069(1)	3.023(1)	3.006(1)
Ln(4)−Se(5)	3.190(1)	3.131(1)	3.071(1)
Ln(4)−Se(6)	3.216(1)	3.209(1)	3.204(1)
Ti(1)−O(2)	1.874(5)	1.876(6)	1.874(5)
Ti(1)−Se(2)	2.569(1)	2.567(1)	2.551(1)
Ti(1)−Se(6) ×2	2.655(1)	2.640(1)	2.623(1)
Ti(1)−Se(3) ×2	2.667(1)	2.653(1)	2.653(1)
Ti(2)−O(3) ×2	1.908(5)	1.909(6)	1.909(5)
Ti(2)−Se(1) ×4	2.680(1)	2.665(1)	2.652(1)
Ti(3)−O(1) ×2	1.941(5)	1.938(6)	1.935(5)
Ti(3)−Se(5) ×4	2.657(1)	2.644(1)	2.635(1)

(28) Mulay, L. N., Boudreaux, E. A., Eds. *Theory and Applications of Molecular Diamagnetism*; Wiley-Interscience: New York, 1976.

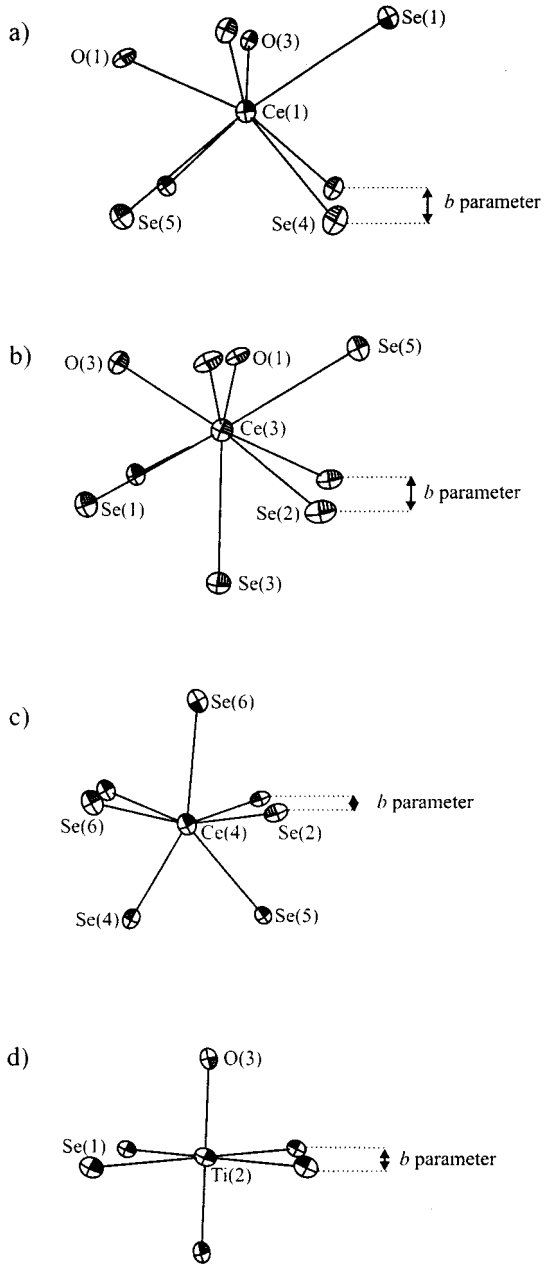

Figure 2. View of the environment of (a) Ln(1), (b) Ln(3), (c) Ln(4), and (d) Ti(2) in $Ce_{3.67}Ti_2O_3Se_6$. Here, and in Figures 3 and 4, the displacement ellipsoids are drawn at the 90% probability level.

The main building units of the structure are motifs derived from trigonal prisms about Ln or octahedra about Ti. The heights of these moieties correspond to the length of *b*, and thus interconnection in the [010] direction occurs by the face sharing of trigonal prisms and Se− Se edge sharing of octahedra.

The crystal structure of $Ce_{3.67}Ti_2O_3Se_6$ (Figure 1) shows successive condensed and expanded slabs stacked along the *a* axis. These are connected through edge-sharing $Ce(3)O_3Se_6$ units. The condensed slabs of composition $^2_\infty[Ce_4Ti_2O_4Se_4Se_{5/2}]$ are constructed from the close packing of $Ce(1)O_3Se_5$, $Ce(3)O_3Se_6$, $Ti(2)O_2Se_4$, and $Ti(3)O_2Se_4$ polyhedra. Within a condensed slab (Figure 3) each TiO_2Se_4 octahedron shares two triangular faces and two edges with four near-neighbor trigonal prisms. The borders of these condensed slabs are infinite planes perpendicular to [010] of alternating Se(5)−Ce(3)-Se(1)−Ce(1) chains. The extended slabs of composition $^2_\infty[Ce_{3.33}Ti_2O_2Se_3Se_{5/2}]$ are constructed from $Ce(2)O_3Se_5$, $Ce(4)Se_7$, and $Ti(1)OSe_5$ polyhedra. Within an extended slab $Ce(2)O_3Se_5$ bicapped trigonal prisms and $Ti(1)Se_5O$ octahedra pack by face sharing and edge sharing to form a large rectangular prism encapsulating O(2) anions. These prisms, which lie in the *ac*-plane, along with the Se(5)−Ce(3)−Se(1)−Ce(1) border define the pseudo-octahedral site about the Ce(4) atom and the vacant trigonal prism of Se atoms (Figure 4). The connection between the different slabs occurs by the sharing of five Se atoms.

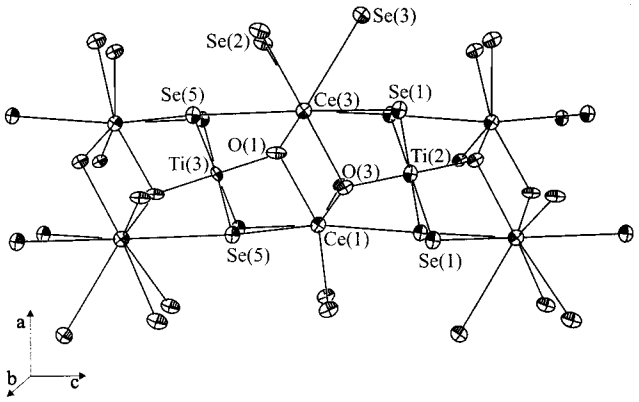

Figure 3. Fragment of the condensed slab in $Ce_{3.67}Ti_2O_3Se_6$.

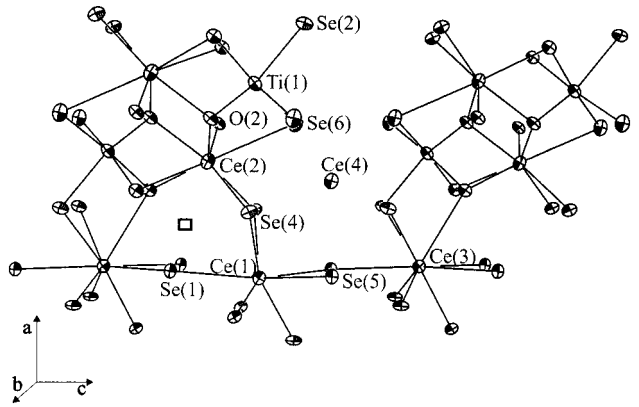

Figure 4. Fragment of the extended slab in $Ce_{3.67}Ti_2O_3Se_6$. Bonds around the Ce(4) atom have been removed for clarity. The square corresponds to a vacant position in a trigonal prism of Se atoms.

The three-dimensional structure of $Ln_{3.67}Ti_2O_3Se_6$ (Ln = Ce, Nd, Sm), built by edge or face sharing of metal-centered polyhedra, results in the following coordination geometries about O and Se. Atoms O(1), O(2), and O(3) are each surrounded by three Ln atoms and one Ti atom in a distorted tetrahedral geometry; atoms Se(1), Se(2), Se(3), and Se(4) are surrounded by five cations in a distorted square-base pyramidal geometry; atoms Se(5) and Se(6) are surrounded by four Ln atoms and two Ti atoms in an irregular octahedral environment.

Since there are no Se−Se bonds in the present structures, the formal oxidation states Se^{2-} and, of course, O^{2-} may be assigned with confidence. The reasonable assignment of Ln^{3+} then leads to equal numbers of Ti^{3+} and Ti^{4+}cations in the structure. Examination of the Ti−Se and Ti−O bond distances (Table 2) does not allow us to assign the two types of

Table 3. Bond Valences[a] of Ti Cations in $Nd_{3.67}Ti_2O_3Se_6$

	Ti(1)	Ti(2)	Ti(3)		Ti(1)	Ti(2)	Ti(3)
Ti^{3+}	3.35	3.31	3.30	Ti^{4+}	3.40	3.41	3.39

[a] Bond valences (γ_{ij}) were calculated from the expression $\gamma_{ij} = \exp[(R_o - d_{ij})/b]$, where $b = 0.37$ Å, $R_o(Ti^{3+}-O) = 1.791$ Å, $R_o(Ti^{4+}-O) = 1.815$ Å, $R_o(Ti-Se) = 2.38$ Å, and d_{ij} are the experimental interatomic distances. See ref 36.

Ti cations to specific crystallographic sites. From the literature for titanium oxides[29−32] one expects Ti^{3+} cations to be in an undistorted octahedral environment with bond distances of about 2.02−2.04 Å whereas one expects Ti^{4+} to be in a distorted octahedral environment with strong bonds of about 1.75 Å and weak bonds of about 2.20 Å in length. Such a distortion about an octahedrally coordinated d^0 ion arises from the bond network as well as electronic effects.[33] Concerning Ti−Se distances, in the present compounds these are slightly longer than that of 2.554(1) Å in $TiSe_2$ (Ti^{4+})[34] and about the same as those in $TlTi_5Se_8$ (Ti^{3+}).[35] The most reasonable assumption is that in the present compounds there is a random distribution of equal numbers of Ti^{3+} and Ti^{4+} cations over the three Ti crystallographic sites. Calculations employing the bond−valence method[36] support this assumption. Table 3 lists results of these calculations for Ti^{3+} and Ti^{4+} in $Nd_{3.67}Ti_2O_3Se_6$. The random distribution of 3d cations in different oxidation states has also been postulated for $La_5V_3O_7S_6$,[7] $La_8Ti_{10}O_4S_{24}$,[14] and $La_{8+x}Ti_{8+y}O_4S_{24}$.[15] A mixture of Ti^{3+} and Ti^{4+} cations over a unique sublattice has not been frequently observed for chalcogenides, whereas it has been commonly described for oxides. In particular, mixed-valence Ti^{3+} and Ti^{4+} have been seen in the nonstoichiometric or doped rare-earth titanium perovskites, which have been extensively studied for their interesting physical properties.[37,38]

Magnetic Properties. Plots of the inverse magnetic susceptibilities vs temperature for $Ce_{3.67}Ti_2O_3Se_6$ and $Nd_{3.67}Ti_2O_3Se_6$ are shown in Figure 5. The ZFC curves show no apparent magnetic ordering. Both compounds follow Curie−Weiss behavior, $\chi^{-1} = (T - \theta_p)/C$, in the temperature range 100−300 K. Below 80 K, these materials deviate from Curie−Weiss behavior and the negative values of the Weiss temperature (Table 4) perhaps indicate antiferromagnetic interactions. But the ZFC and FC curves measured for $Nd_{3.67}Ti_2O_3Se_6$ are similar and the magnetization vs magnetic field measured at 5 K is linear with no saturation moment reached at 5 T. Thus, the paramagnetic regime is confirmed down to 5 K. Consequently, the observed deviations may result from a crystal-field splitting of

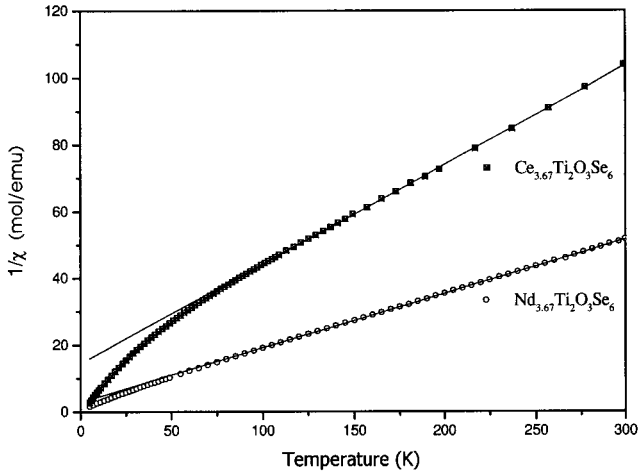

Figure 5. χ^{-1} versus T for $Ce_{3.67}Ti_2O_3Se_6$ and $Nd_{3.67}Ti_2O_3Se_6$; the solid lines correspond to the Curie−Weiss fits.

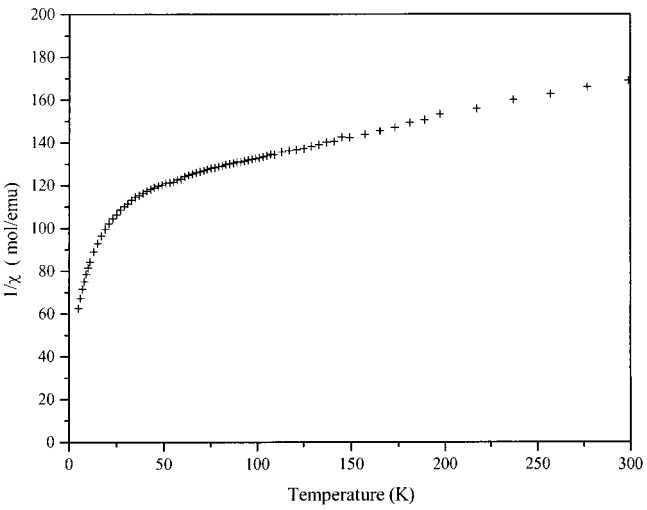

Figure 6. χ^{-1} versus T for $Sm_{3.67}Ti_2O_3Se_6$.

Table 4. Experimental and Calculated Magnetic Data.

compound	θ_p (K)	C_{exp} (emu K mol^{-1})	μ_{eff}(exp) (μ_B)	μ_{eff}(calc) (μ_B)
$Ce_{3.67}Ti_2O_3Se_6$	−48.5(5)	3.369(7)	5.19(3)	5.16
$Nd_{3.67}Ti_2O_3Se_6$	−17.4(2)	6.151(6)	7.01(3)	7.14

the $J = {}^5/_2$ and $J = {}^9/_2$ ground states of the Ce^{3+} and Nd^{3+} cations, respectively.

The experimentally determined values of the Curie constant C (Table 4) deviate slightly from the summation of the ideal free-ion values for Ce^{3+} (0.806 emu K mol^{-1}) and Nd^{3+} (1.638 emu K mol^{-1}).[39] This suggests that the magnetic susceptiblies are composed of contributions from both Ln^{3+} and Ti^{3+} cations. Since the shortest Ti−Ti distances are about 3.8 Å and the Ti^{3+} cations are diluted over the Ti sites, the d^1 electrons are localized and a calculated spin-only Curie constant of 0.37 emu K mol^{-1} may be taken for Ti^{3+}. The effective magnetic moments calculated for a model of 3.67 Ln^{3+} and 1.00 Ti^{3+} compare reasonably well with the experimental values (Table 4). But given the small value of the Curie constant for Ti^{3+} versus those for Ln^{3+}, the magnetic measurements do not allow confirmation of

(29) MacLean, D. A.; Ng, H.-N.; Greedan, J. E. *J. Solid State Chem.* **1979**, *30*, 35−44.
(30) Robinson, W. R. *J. Solid State Chem.* **1974**, *9*, 255−260.
(31) Scheunenmann, K.; Müller-Buschbaum, H. *J. Inorg. Nucl. Chem.* **1975**, *37*, 2261−2263.
(32) Evans, H. T., Jr. *Acta Crystallogr.* **1961**, *14*, 1019−1026.
(33) Kunz, M.; Brown, I. D. *J. Solid State Chem.* **1995**, *115*, 395−406.
(34) Riekel, C. *J. Solid State Chem.* **1976**, *17*, 389−392.
(35) Klepp, K.; Boller, H. *J. Solid State Chem.* **1983**, *48*, 388−395.
(36) Brese, N. E.; O'Keeffe, M. *Acta Crystallogr., Sect. B* **1991**, *47*, 192−197.
(37) Amow, G.; Greedan, J. E. *J. Solid State Chem.* **1996**, *121*, 443−450.
(38) Eylem, C.; Ju, H. L.; Eichhorn, B. W.; Greene, R. L. *J. Solid State Chem.* **1995**, *114*, 164−173.
(39) Kittel, C. *Introduction to Solid State Physics*, 6th ed.; Wiley: New York, 1986.

the number of Ti^{3+} cations per formula unit that is dictated by charge balance.

The temperature dependence of the inverse magnetic susceptibility of $Sm_{3.67}Ti_2O_3Se_6$, displayed in Figure 6, reveals paramagnetic behavior down to 5 K. The curved shape, which is similar to that observed for Sm_2Se_3 with the defect Th_3P_4 structure type[40] and for the misfit layer compound $(SmS)_{1.25}(TiS_2)_2$,[41] is characteristic of the Van Vleck paramagnetic ion Sm^{3+}, for which a mixture of several energy levels occurs at high-temperature, rendering the effective magnetic moment temperature dependent.[42] Therefore, no Curie−Weiss constants can be derived from these data.

Acknowledgment. This research was supported by the U.S. National Science Foundation under Grant DMR 97-09351. This work made use of Central Facilities supported by the MRSEC program of the National Science Foundation (DMR-9632472) at the Materials Research Center of Northwestern University. We thank S. Shafaie at the Analytical Services Laboratory of Northwestern University for his help in the ICP-AES measurements.

Supporting Information Available: X-ray crystallographic files in CIF format for the structure determinations of $Ln_{3.67}Ti_2O_3Se_6$ (Ln = Ce, Nd, Sm). This material is available free of charge via the Internet at http://pubs.acs.org.

CM000203M

(40) Grundmeier, T.; Heinze, T.; Urland, W. *J. Alloys Compd.* **1997**, *246*, 18−20.

(41) Cario, L.; Meerschaut, A.; Lafond, A.; Rouxel, J. *Mater. Res. Bull.* **1996**, *31*, 1307−1316.

(42) Van Vleck, J. H. *The Theory of Electric and Magnetic Susceptibilities*; Oxford University Press: London, 1932.